

Carriers of 4964 and 6196 diffuse interstellar bands and environments dominated by either CH or CH⁺ molecules

Weselak¹, T., Galazutdinov^{2,3}, G.A., Sergeev⁴, O., Godunova⁴, V., Kołos⁵, R., Krelowski⁶, J.

¹ Institute of Physics, Kazimierz Wielki University, Weyssenhoffa 11, 85-072 Bydgoszcz, Poland e-mail: towes@gazeta.pl

² Instituto de Astronomia, Universidad Catolica del Norte, Av. Angamos 0610, Antofagasta, 1270709 Chile

³ Pulkovo Observatory, Pulkovskoe Shosse 65, Saint-Petersburg 196140, Russia e-mail: runizag@gmail.com

⁴ International Center for Astronomical, Medical and Ecological Research
Postal code and address: 27 Zabolotnoho Str., Kyiv 03680 Ukraine
e-mail: sergeev@terskol.com; godunova@mao.kiev.ua

⁵ Institute of Physical Chemistry, Polish Academy of Sciences
Kasprzaka 44, 01-224 Warsaw, Poland
e-mail: robert.kolos@ichf.edu.pl

⁶ Center for Astronomy, Nicolaus Copernicus University, Grudziądzka 5, Pl-87-100 Toruń, Poland
e-mail: jacek@astri.uni.torun.pl

Received Month Day, Year

ABSTRACT

The analysis of radial velocities of interstellar spectral features: CH, CH⁺ as well as 4964 and 6196 diffuse interstellar bands, seen in spectra of HD 151932 and 152233, suggests that carrier of the former is spatially correlated with CH while that of the latter – with CH⁺. A further analysis, done in this paper and based on the sample of 106 reddened OB stars, partly confirms this suggestion, showing that the CH column density correlates indeed much better with the equivalent width of the 4964 DIB than with that of the 6196 DIB. However, the strengths of the 6196 DIB correlate only marginally better with CH⁺ than with CH.

Key words:

ISM: molecules

Introduction

Diffuse interstellar bands (DIBs) are numerous narrow to broad absorption features mostly found in the visual and near infrared (4,000-10,000Å) spectra of early type OB–stars. Despite many observational efforts (Herbig 1995, Galazutdinov et

al. 2000, Weselak et al. 2000, Hobbs et al. 2008, and references therein), DIBs remain one of the longest standing puzzles in stellar spectroscopy. Since their discovery (Heger 1922) not a single DIB carrier has been identified, although many possible candidates were proposed (Herbig 1995). The coincidence of a weak DIB at 5069 Å with the gas-phase absorption of the linear, centrosymmetric hydrocarbon chain cation HCCCCCH^+ has been recently reported by Krelowski et al. (2010). However, this identification, as well as the recent assignment of two broad diffuse bands near 4882 and 5450 Å to the propadienylidene ($\text{l-C}_3\text{H}_2$) molecule (Maier et al., 2011a) have been disputed (Krelowski et al. 2011; Maier et al. 2011b) and remain uncertain. Recent results of Ehrenfreund et al. (2002), Cox and Patat (2008) proved the existence of DIBs and molecular features in spectra of LMC/SMC and M100 stars, respectively. However, measurements of weak interstellar features are hindered by relatively low signal-to-noise (S/N) inside their profiles.

The molecular origin of at least some DIBs seems likely, their profiles being often complex and reminiscent of rotational envelopes in molecular spectra (Sarre et al. 1995a, Kerr et al. 1998). The 6614 DIB contains three main components that have the appearance of unresolved P, Q and R branches of an electronic transition of a large molecule (see Herzberg 1950). A more or less similar pattern is observed also in the case of 5797 DIB, the strength of which correlates tightly with the CH column density (Weselak et al. 2008b). This correlation supports also the idea that carriers of some DIBs are molecules. Another important piece of evidence is that the width of certain DIB can depend on the temperature within an interstellar cloud - as shown by Kaźmierczak et al. (2009) who have found a correlation between the FWHM of the 6196 DIB and the rotational temperature of the homonuclear C_2 molecule. An important conjecture here is that some of the DIBs, namely those sensitive to temperature of the environment, may originate in centrosymmetric molecules, as the lack of electric dipole moment slows down the rotational relaxation (see Bernath 2005).

Methylidyne (CH), first identified in the ISM by McKellar (1940), is closely related to molecular hydrogen (H_2), as already shown by Mattila (1986) and Weselak et al. (2004) and also with OH (Weselak et al. 2009b, 2010b). The abundances of CH molecule are also well correlated with those of NH (Weselak et al. 2009c). On the other hand, the column density of the corresponding cation, CH^+ , correlates very poorly with that of H_2 - indicating no relation between the abundances of these two molecules (Weselak et al. 2008a). The formation and existence of CH^+ in the ISM remains an unsolved problem (van Dishoeck and Black 1989, Gredel et al. 1993, Sheffer et al. 2008 and references therein). One can argue that environments dominated by the CH molecule (i.e. regions where it is much more abundant than CH^+), and those where CH^+ dominates, are well separated in space. This conclusion is grounded in the publication of Allen (1994) which demonstrates that radial velocities of CH and CH^+ may differ by as much as 7.3 km/s.

Spectral observations of highly-reddened early type stars offer an excellent op-

portunity to probe large column densities of gas along diverse lines of sight, to derive physical parameters of corresponding environments and eventually unveil the nature of DIB carriers. Identified and unidentified interstellar spectral features should share the radial velocities if they originate in the same environments. In such a case, their intensities should be correlated as well.

The aim of this work is to present the relations between the column densities of simple diatomic molecules CH and CH^+ and the equivalent widths of two narrow DIBs: 4964 and 6196 Å. It is certainly important to specify the physical parameters of environments which host the DIB carriers. It may shed some light on the conditions facilitating the formation/preservation of DIB carriers. This is particularly interesting in the context of interstellar CH and CH^+ synthesis paths, presented by Federman et al. (1982) and by Zsargó and Federman (2003).

1. The observational data

The observations¹ were obtained during several runs spanning the period 1999–2007, using BOES (b), FEROS (f), UVES (U) and HARPS (H) échelle spectrographs. We also retrieved fully reduced UVES (u) spectra of several objects listed in Table 1 from the "Library of High-Resolution Spectra of Stars across the Hertzsprung-Russell Diagram" (Bagnulo et al. 2003, <http://www.sc.eso.org/santiago/uvespop>). Spectra were reduced using MIDAS and IRAF, as well as our own DECH code (Galazutdinov 1992), which provides all standard procedures for image and spectra processing. The DECH code was employed during the final data analysis.

The usage of several different software data reduction packages allows us to get better control over proper dark subtraction, flatfielding, or excision of cosmic ray spikes. We measured the equivalent widths of selected features using a Gaussian fit (see Weselak et al. 2009a) in the spectra obtained using different instruments. Some of our targets were observed several times which allowed for the estimation of repeatability (it is not likely that two observers make the same error). In such cases the measurements were averaged. In the case of spectral features that were unsaturated ($EW < 20 \text{ mÅ}$), the following relation were applied (Weselak et al. 2009a) to obtain the column density (in cm^{-2}):

$$N = 1.13 \times 10^{20} (EW/f\lambda^2),$$

where EW is equivalent width of the line, λ its wavelength (both in Å), and f – its oscillator strength.

We calculated the column density of the CH^+ cation adopting, for an unsaturated 4232 Å band, the oscillator strength $f=0.00545$ reported by Larsson and Siegbahn

¹Based on observations made with ESO Telescopes at the La Silla or Paranal Observatories under programs 71.C-0367(A), 073.D-0609(A), 074.D-0300(A), 075.D-0369(A), 076.C-0431(B) and 082.C-0566(A).

(1983). The same procedure has been applied in a former study by Weselak et al. (2008a). Whenever the 4232 Å band was saturated, measurements of the CH⁺ feature at 3957 Å were performed, using its recently obtained f -value of 0.00342 (Weselak et al. 2009a). When estimating the column density of CH⁺, we only used the bands of the total equivalent width lower than 20mÅ. In the case of two objects where Doppler-splitting is evident (HD 152235 and 168607), we also made use of the 3957 Å band to estimate the column densities. In the case of HD 34078, we relied on the unsaturated CH⁺ (2, 0) band at 3745Å, with its recently published f -value of 0.00172 (Weselak et al. 2009a).

In the case of CH molecule we calculated column density based on unsaturated CH A–X band at 4300 Å adopting recent f -value of 0.00506 (Weselak et al. 2014). When the 4300 Å feature was saturated we used both CH B–X bands at 3886 and 3890 Å (f -values equal to 0.00320 and 0.00213, respectively – see Weselak et al. 2014). The CH B–X bands at 3886 and 3890 Å were used in the case of HD's: 34078, 147889, 154368 and 204827 respectively.

2. Results

For this project we choose a sample of 106 reddened OB stars, for which we collected the echelle spectra featuring CH and CH⁺ bands, as well as the DIBs at 4964 and 6196 Å. For each line of sight. Tables 1 and 2 list a stellar HD/ BD number (observed by b – BOAO, f – FEROS, H – HARPS, U – UVES), spectral type, luminosity class, colour excess $E(B-V)$ (in magnitudes), as well as the column densities of CH⁺ and CH molecules (in 10^{12} cm^{-2} units, together with corresponding error estimates), and finally the equivalent widths (W_λ 's) of diffuse bands, with their standard deviations. In Figure 1 we present, in the radial velocity scale, the CH and CH⁺ features, as seen in a very high S/N ratio (2,500) spectrum of HD 149757 (ζ Oph). It is evident that radial velocities of both species are identical. At the bottom of this figure we also show the two narrow DIBs at 4963.85 and 6195.97 Å in the spectrum of HD 23180, taken from the survey of Galazutdinov et al. (2000). A weak feature at 6194.76 Å can be seen in the vicinity of 6196 DIB. Also the radial velocities of 4964 and 6196 DIBs do not differ, as far as their asymmetric profiles allow for central wavelengths measurements.

To determine the DIB radial velocities we have used the rest wavelength velocity frame based on the KI line at 7698.974 Å (Galazutdinov et al. 2000) toward HD 23180 where radial velocities of all identified interstellar features are the same. This method allows us to measure radial velocities of diffuse bands and of narrow interstellar features with a very low uncertainty, smaller than 0.3 km/s (see Fig. 1). HD 149757 is a moderately reddened, popularly observed object, with no Doppler splittings of interstellar features. The above statement is supported by the observations of CH B-X lines (centered near 3886 and 3890 Å) and of the feature near 3957 Å, belonging to the CH⁺ cation, which proved useful for column density

derivation when saturation affected stronger bands (Weselak et al. 2008a, 2008b). We observed ζ Oph using UVES and HARPS spectrographs, and the result is the same in both cases: no Doppler shift of any feature, relative to any other one, is observed toward this target.

It is well known that the CH^+ cation needs different interstellar conditions than CH to be formed (Federman 1982). In many cases CH^+ features are Doppler-split, while those of CH are not (see Pan et al. 2004). However, there are also lines of sight where we observed the splitting in both CH and CH^+ bands. In Figure 2 we present a fragment of HD 152233 spectrum, measured with HARPS, with CH and CH^+ (4300 and 4232 Å, respectively) features plotted in the radial velocity scale. The CH^+ line is apparently Doppler split, and contains two components; conversely, only one component is detected for the neutral CH molecule. At the bottom of Fig. 2 we present the spectral region of 4964 and 6196 DIBs, in the same velocity scale. Intrinsic DIB wavelengths were those of Galazutdinov et al. (2008). In the case of broader DIBs (see Fig. 1), the error of radial velocity measurements is not larger than 1-2 km/s. It is evident that the 6196 DIB shares its radial velocity with the blue-shifted (-7.6 ± 0.4 km/s) component of the CH^+ line, while the 4964 DIB shares the radial velocity with CH. A similar effect can be observed in the UVES spectrum of HD 151932, with the blue-shift of CH^+ equal to -6.1 ± 0.2 km/s (Fig. 3).

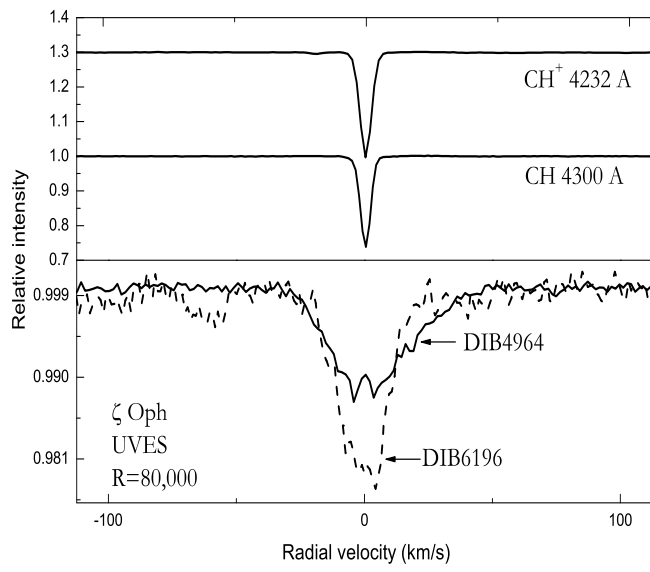


Figure 1: Top panel: CH A-X and CH⁺ A-X lines centered near 4300 and 4232 Å, respectively, as seen in the spectrum of HD 149757. Common radial velocity scale. Bottom panel presents the DIBs at 4963.85 and 6195.97 Å (Galazutdinov et al. 2000), in the same radial velocity scale. A weak DIB at 6194.76 Å can be discerned. Difference in radial velocities is not higher than 0.3 km/s.

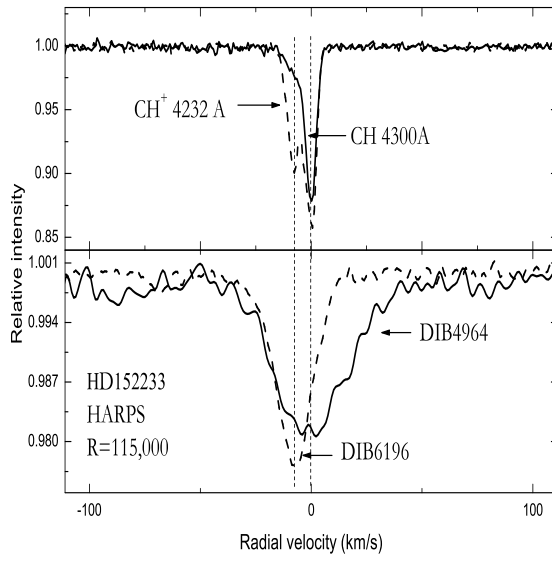


Figure 2: The 6196 DIB is shown sharing the velocity of the second component of CH⁺, while 4964 DIB remains at the position of CH. The depth of the 6196 DIB is scaled down by a factor of 2. It is evident that the 6196 DIB shares its radial velocity with the blue-shifted (-7.6 ± 0.4 km/s), weaker component of the CH⁺ line.

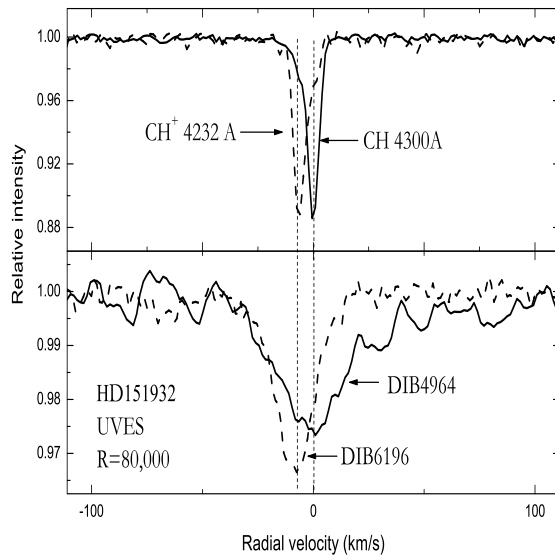


Figure 3: Same as Fig. 2 but for a different target observed with another instrument. The depths of 4300 Å CH line and of 6196 DIB are scaled down by a factor of 2. The 4964 DIB shares the radial velocity with CH in the UVES spectrum of HD 151932, with the blue-shift of CH⁺ equal to -6.1 ± 0.2 km/s.

Such telltale Doppler shift analyses can at present, unfortunately, not be accomplished for a statistically meaningful sample of cases, given the fact that velocity differences between CH and CH^+ are usually very small. Therefore, the only reliable possibility of investigating the spacial relationships between DIB carriers and simple molecules is to correlate DIB strengths with molecular column densities derived for an extensive sample of sight lines. Figure 4 shows such relations for CH versus either 4964 or 6196 DIBs. It is clear that the 4964 DIB is very well correlated with the column density of CH, while for 6196 DIB the similar correlation is moderate (correlation coefficients equal 0.86 and 0.48, respectively).

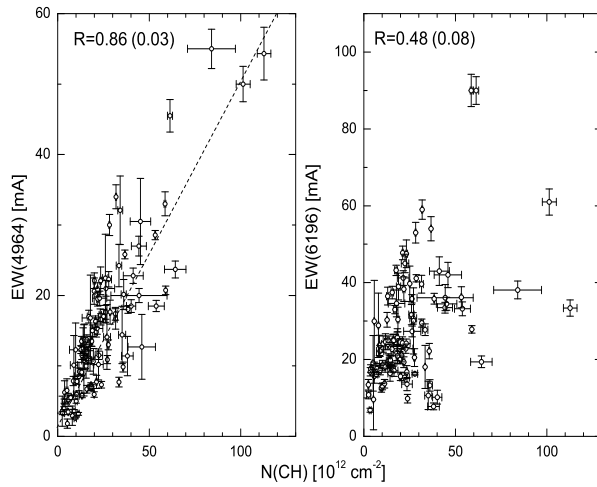


Figure 4: Equivalent widths of 4964 and 6196 DIBs plotted vs. the column density of CH (correlation coefficients equal 0.86 and 0.48, respectively). Very good relation between equivalent widths of 4964 DIB and column densities of CH molecule is presented with dotted line.

Very good relation with correlation coefficient equal to 0.86, seen in Fig. 4 proves that the carrier of 4964 DIB occupies the same regions of translucent clouds as the neutral methyldiyne molecule. It also means that 74 % (0.86×0.86) of the total variation in equivalent width of the 4964 DIB can be explained by the linear relationship between equivalent widths of the 4964 DIB and column densities of CH molecule seen in Fig. 4. This molecule, on the other hand, does not seem to share the environment with a 6196 DIB carrier. Fig. 5 shows another piece of evidence: the column density of CH^+ correlates weakly with the strength of 4964 DIB (correlation coefficient equal to 0.47), and only marginally better with that of 6196 DIB with the calculated correlation coefficient equal to 0.68. Of note, since CH and CH^+ are not well mixed within the interstellar clouds, their column density ratio cannot serve as a useful physical parameter characterizing individual

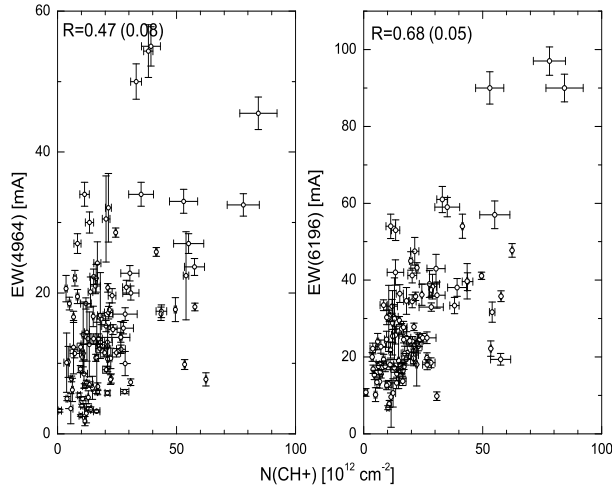


Figure 5: Correlation of both 4964 and 6196 DIBs with column density of CH^+ (correlation coefficients equal to 0.47 and 0.68, respectively). Note better relation between equivalent widths of 6196 DIB and column densities of CH^+ molecule suggested by radial velocity shift presented in Figs. 2 and 3.

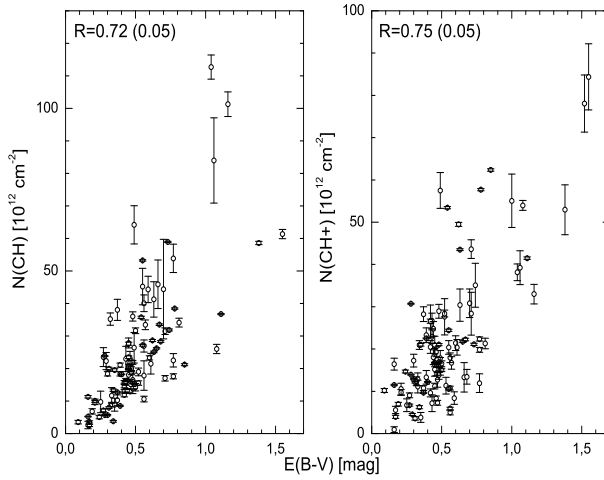


Figure 6: Column densities of both CH and CH^+ correlate to a similar degree with $E(B-V)$ (in magnitudes). Moderate relations with correlation coefficients equal to 0.72 and 0.75, respectively.

lines of sight. It seems also that a predictive value of the colour excess $E(B-V)$, in the discussed contexts, is very doubtful (Fig. 6). Both CH and CH^+ are correlated

with $E(B-V)$ to a similar, moderate, degree with correlation coefficients equal to 0.72 and 0.75, respectively.

3. Conclusions

The above considerations lead us to infer the following conclusions:

1. The 4964 DIB carrier is spatially correlated with neutral methylidyne; this is confirmed by both the analysis of Doppler velocities and by the correlation of $N(\text{CH})$ vs. $\text{EW}(4964)$. The 6196 DIB, which seemed related to CH^+ based on Doppler shifts, correlates only marginally better with this species than with 4964, in terms of $N(\text{CH}^+)$ vs. $\text{EW}(6196)$.
2. The equivalent widths of discussed diffuse bands, as well as the molecular column densities derived here, all correlate reasonably well with $E(B-V)$, which makes the latter parameter not very useful in case of finding DIB carriers originating in different interstellar environments.

The good correlation of CH with the 4964 DIB suggests the existence of other, similar connections between simple molecules and DIBs. However, in order to show the division of DIBs between different environments, one needs the spectra of very high S/N ratio. It could be very rewarding to check for the relations between the strong DIBs and the interstellar molecules such as C_2 or CO - based on new samples, coming from homogeneous measurements. However, a majority of DIBs show the profiles too broad to allow for a Doppler shift analysis. It is certainly important to collect more spectra of the high signal-to-noise ratio, offering the correct column density values for simple diatomics, and thus indicating the possible relations of observed molecules to DIBs carriers. In any case it seems to be of basic importance to relate the origin of diffuse bands to certain interstellar environments, defined by specific physical parameters, the latter available from analyzes of identified atomic and/or molecular features.

Acknowledgements. JK and TW acknowledge the financial support provided by the Polish National Center for Science for the period 2012 - 2015 (grant UMO-2011/01/BST2/05399). The authors benefited from the funds of the Polish-Ukrainian PAS/NASU joint research project No. 21(2009-2011). We are grateful for the assistance of the ESO and BOAO observatories staff members.

REFERENCES

- Allen, M.M., 1994, *ApJ*, 424, 754
 Bagnulo, S., Jehin, E., Ledoux, C., Cabanac, R., Melo, C., Gilmozzi, R., The ESO Paranal Science Operations Team, 2003, *Msngr*, 114, 10
 Bernath, P.: 2005, in: *Spectra of Atoms and Molecules* (Oxford Univ. Press)

- Cox, N.L.J. and Patat, F., 2008, A&A, 485, 9
- Crane, P., Lambert, D.L., Sheffer, Y., 1995, ApJS, 99, 107
- Ehrenfreund, P., Cami, J., Jiménez-Vincente, J., et al., 2002, A&A, 576, 117
- Federman, S.R., 1982, ApJ, 257, 125
- Galazutdinov, G.A., 1992, Prep. Spets. Astrof. Obs., No 92.
- Galazutdinov, G.A., Musaev, F.A., Krełowski, J., Walker, G.A.H., 2000, PASP, 112, 648
- Galazutdinov, G. A., Lo Curto, G., Krełowski, J., 2008, ApJ, 682, 1076.
- Gredel, R., van Dishoeck, E.F., Black, J.H., 1993, A&A, 269, 477
- Heger, M.L., 1922, Lick Obs. Bull. 10, 146
- Herbig, G. H., 1975, ApJ, 196, 129
- Herbig, G. H., 1995, ARAA, 33, 19
- Herzberg, G.: 1950, Molecular Spectra and Molecular Structure, Vol. 1: Spectra of Diatomic Molecules (New York: D. Van Nostrand Co.)
- Hobbs, L. M., York, D. G., Snow, T. P., Oka, T., Thorburn, J. A., Bishof, M., Friedman, S. D., McCall, B. J., Rachford, B., Sonnentrucker, P., Welty, D. E., 2008, ApJ, 680, 1256
- Jenniskens, P., Desert, F., -X., 1994, A&AS, 106, 39
- Kaźmierczak, M., Gnaciński, P., Schmidt, M. R., Galazutdinov, G., Bondar, A., Krełowski, J., 2009, 498, 785
- Kerr, T.H., Hibbins, R.E., Fossey, S.J., Miles, J.R., Sarre, P.J., 1998, ApJ, 495, 941
- Krełowski J., Beletsky Y., Galazutdinov G.A., Kołos R., Gronowski M., LoCurto G., 2010, ApJ, 714, L64
- Krełowski, J., Ehrenfreund, P., Foing, B.H., Snow, T.P., Weselak, T., Tuairisg, S.Ó, Galazutdinov, G.A., Musaev, F.A., 1999, A&A, 347, 235
- Krełowski, J., Galazutdinov, G., Kołos, R., 2011, ApJ, 735, 124
- Larsson M., Siegbahn P.E.M., 1983, Chem. Phys. 76, 175
- Maier, J.P., Walker, G.A.H., Bohlender, D.A., Mazzotti, F.J., Raghunandan, R., Fulara, J., Garkusha, I., & Nagy, A., 2011, ApJ, 726, 41
- Maier, J.P., Chakrabarty, S., Mazzotti, F. J., Rice, C. A., Dietsche, R., Walker, G. A. H., Bohlender, D. A., 2011, ApJ, 729, 20
- Mattila, K., 1986, A&A, 160, 157
- McKellar, A., 1940, PASP, 52, 187
- Pan, K., Federman, S.R., Cunha, K., Smith, V.V., Welty, D.E., 2004, ApJS, 151, 313
- Sarre, P.J., Miles, J.R., Kerr, T.H., Hibbins, R.E., Fossey, S.J., Sommerville, W.B., 1995a, MNRAS, 277, 41
- Sheffer, Y., Rogers, M., Federman, S.R., Abel, N.P., Gredel, R., Lambert, D.L., Shaw, G., 2008, ApJ, 687, 1075
- Thorburn, J. A., Hobbs, L. M., McCall, B. J., Oka, T., Welty, D. E., Friedman, S. D., Snow, T. P., Sonnentrucker, P., York, D. G., 2003, ApJ, 584, 339
- van Dishoeck, E.F., & Black, J.H., 1989, ApJ, 340, 273
- Weselak, T., Schmidt, M., Krełowski, J., 2000, A&AS, 142, 239
- Weselak, T., Galazutdinov, G.A., Musaev, F.A., Krełowski, J., 2004, A&A, 414, 949
- Weselak, T., Galazutdinov, G.A., Musaev, F.A., Krełowski, J., 2008a, A&A, 479, 149
- Weselak, T., Galazutdinov, G.A., Musaev, F.A., Krełowski, J., 2008b, A&A, 484, 381
- Weselak, T., Galazutdinov, G.A., Musaev, F.A., Beletsky, Y., Krełowski, J., 2009a, A&A, 495, 189
- Weselak, T., Galazutdinov, G.A., Beletsky, Y., Krełowski, J.: 2009b, A&A, 499, 783
- Weselak, T., Galazutdinov, G.A., Beletsky, Y., Krełowski, J.: 2009c, MNRAS, 400, 392
- Weselak, T., Galazutdinov, G.A., Beletsky, Y., Krełowski, J.: 2010b, MNRAS, 402, 1991
- Weselak, T., Galazutdinov, G.A., Gnaciński, P., Krełowski, J.: 2014, AcA, 64, 277
- Zsargó, J., Federman, S.R., 2003, ApJ, 589, 319

Table 1: Observational and measurement data. Are given: HD/BD number (b – BOAO, f – FEROS), Spectral type / Luminosity class, E(B-V) (in magnitudes), column densities (in 10^{12} cm^{-2}) of the CH^+ and CH molecules with error in each case, equivalent widths (in mÅ) of the 4964 and 6196 DIBs with error in each case.

HD/BD	Sp/L	E(B-V)	N(CH^+)	σ	N(CH)	σ	EW(4964)	σ	EW(6196)	σ
23180 b	B1III	0.27	6.71	0.23	23.52	2.91	16.6	0.8	13.6	1.7
24398 b	B1Iab	0.29	4.51	0.23	22.30	2.61	10.2	2.2	15.3	1.2
24534 b	O9.5pe	0.56	4.98	0.58	40.09	2.57	18.5	0.9	10.2	1.8
25638 b	B0III	0.66	13.31	3.47	31.40	7.47	12.7	4.6	42.0	3.3
27778 b	B3V	0.37	7.58	0.58	29.46	3.22	11.4	2.8	7.8	0.9
34078 b	O9.5Ve	0.49	57.5	4.23	64.20	5.88	23.7	1.2	19.4	1.5
45314 f	O9:pe	0.43	7.18	1.97	15.44	0.60	11.4	0.6	22.7	1.7
46150 f	O6e	0.46	15.16	1.50	12.97	0.58	13.5	0.7	36.5	2.3
46223 f	O5e	0.48	28.93	1.62	21.88	0.60	20.8	1.0	38.3	3.2
46573 f	O7	0.63	30.38	3.80	41.26	5.44	22.8	1.1	43.0	3.7
47432 f	O9.5III	0.42	9.61	0.93	11.86	0.56	9.2	0.5	24.6	2.1
48434 f	B0III	0.21	10.53	1.39	10.09	0.52	5.0	0.3	13.0	0.9
75149 f	B3Ia	0.39	13.31	1.62	9.14	0.65	7.0	0.4	25.7	2.3
80558 f	B6Iae	0.60	21.41	1.74	23.28	0.64	17.2	0.9	47.5	3.6
93130 f	O6	0.56	5.90	0.35	10.60	0.87	7.8	0.4	24.0	2.1
94367 f	B9Ia	0.17	3.94	0.35	3.57	0.35	5.0	0.3	16.8	1.1
99264 f	B2IVV	0.27	9.03	0.58	7.12	0.43	5.5	0.3	17.6	1.4
99872 f	B3V	0.34	20.95	1.04	13.35	0.37	5.8	0.3	19.6	1.9
101191 f	O8	0.37	28.24	1.74	10.25	1.67	6.0	0.3	18.5	1.3
101205 f	O8v	0.33	12.85	1.50	8.92	0.65	3.6	0.2	17.2	1.2
101223 f	O7	0.45	11.23	0.69	18.03	1.64	6.8	0.3	21.8	2.1
104841 f	B2IV	0.09	10.18	0.46	3.49	0.54	4.0	0.2	6.8	0.5
110432 f	B2pe	0.48	16.09	0.46	16.51	2.07	10.8	0.5	17.1	1.5
116072 f	B2.5Vn	0.21	9.72	0.69	9.56	0.64	2.6	0.1	12.6	1.1
141637 f	B1.5V	0.16	0.93	0.69	2.61	1.15	3.3	0.2	10.8	1.0
147888 f	B3/B4V	0.46	8.33	0.58	21.84	0.57	19.5	1.0	19.3	1.4
147932 f	B5V	0.47	7.29	0.58	19.97	0.57	22.1	1.1	15.6	1.1
147934 f	B2V	0.45	15.16	1.62	27.86	1.53	22.3	1.1	16.3	0.3
148379 f	B2Iab	0.77	19.79	0.58	22.53	2.06	11.5	0.6	45.0	2.4
148688 f	B1Ia	0.52	27.63	4.28	18.98	1.18	15.0	0.8	39.0	3.5
148937 b	O6e	0.61	20.39	1.85	21.47	3.18	15.3	0.8	41.2	1.9
149404 b	O9Ia	0.71	43.63	2.20	31.50	1.02	17.4	0.9	39.6	2.3
150136 b	O5	0.42	20.49	1.50	13.14	0.36	9.1	0.5	24.0	1.3
150168 b	B1Iab/Ib	0.16	16.43	1.39	11.31	0.38	3.2	0.2	13.7	1.1
152076 b	B0.5III	0.43	22.92	1.62	22.94	3.86	19.6	1.0	22.8	1.2
152218 b	O9V	0.45	18.29	1.85	20.70	0.66	16.3	0.8	21.1	1.7
152219 b	O9IV	0.44	24.77	1.74	13.27	0.60	11.5	0.6	25.0	1.1
152234 b	B0.5Ia	0.42	26.58	3.80	15.88	0.43	13.7	0.7	25.0	1.5
152246 b	O9Ib	0.44	18.06	1.74	16.31	0.31	13.0	0.7	25.0	1.6
152314 b	B0.5Iab	0.39	23.26	1.74	21.05	0.66	14.8	0.7	24.3	1.6
152667 b	B0.5Iae	0.47	12.73	1.74	18.64	0.50	13.5	0.7	30.4	3.2
154090 b	B1Iae	0.45	20.95	2.08	27.63	0.45	13.0	0.7	20.5	2.3
164794 b	O4V	0.33	11.11	1.50	11.67	2.47	8.5	2.0	18.0	1.3
165688 b	WN	1	55.06	6.33	—	—	27.0	1.4	57.0	3.6
166734 b	O8e	1.38	52.95	5.91	58.60	0.52	33.0	1.7	90.0	4.2
168075 b	O7V	0.74	35.07	5.21	31.85	0.30	34.0	1.7	59.0	2.5
168137 b	O8.5V	0.68	13.43	1.74	28.29	0.28	30.0	1.5	53.0	2.7
168607 b	B9Ia	1.55	84.38	7.80	61.36	1.41	45.5	2.3	90.0	3.6
168625 b	B6Ia	1.52	78.05	6.75	—	—	32.5	1.6	97.0	3.7
184915 b	B0.5III	0.19	6.94	0.46	6.85	0.81	—	—	16.1	0.6
190603 b	B1.5Iae	0.71	28.36	5.06	17.00	0.85	17.0	0.9	33.0	1.1
203064 b	O8V	0.25	6.71	1.50	9.75	3.30	12.3	3.8	18.3	0.5
203938 b	B0.5IV	0.7	30.80	3.38	34.20	15.30	20.0	1.0	36.1	3.4
204827 b	B0V	1.06	39.24	4.01	84.00	13.10	55.0	2.8	38.1	2.3
206165 b	B2Ib	0.46	19.33	1.16	23.09	2.21	—	—	24.2	1.1
206267 b	O6	0.49	11.33	2.08	26.40	4.71	21.0	1.1	27.3	1.4
207198 b	O9II	0.55	20.37	1.62	35.64	5.62	30.5	6.1	34.5	1.7
207538 b	B0V	0.59	8.39	1.50	44.34	4.07	27.0	1.4	33.5	1.4
208501 b	B8Ib	0.77	11.92	2.20	53.86	4.36	18.5	0.8	33.2	1.8
209481 b	O9V	0.35	3.82	1.16	8.87	2.01	10.1	4.2	22.2	1.4
210839 b	O6e	0.56	10.76	0.46	26.93	1.86	14.1	4.6	30.7	1.5
213087 b	B0.5Ibe	0.56	17.94	1.16	17.84	4.50	16.8	6.1	34.6	3.5
326331 b	B	0.3	17.25	1.50	18.38	0.68	13.5	0.7	20.9	1.9
BD134927 f	O7II	1.16	32.99	2.31	101.3	3.80	50.0	2.5	61.0	3.4
BD134930 f	O9.5V	0.53	11.34	1.97	—	—	34.0	1.7	54.0	3.2
CPD417733 b	O9III	0.49	17.82	1.85	14.42	0.65	12.1	0.6	19.4	1.5
CPD417735 b	O9V	0.43	26.62	1.85	15.97	0.97	12.0	0.6	18.0	1.3

Table 2: Observational and measurement data (continued). Are given: HD/BD number (H – HARPS, U – UVES), Spectral type / Luminosity class, E(B-V) (in magnitudes), column densities (in 10^{12} cm^{-2}) of the CH^+ and CH molecules with error in each case, equivalent widths (in mÅ) of the 4964 and 6196 DIBs with error in each case.

HD/BD	Sp/L	E(B-V)	N(CH^+)	σ	N(CH)	σ	EW(4964)	σ	EW(6196)	σ
144217 H	B0.5V	0.17	5.582	0.85	2.481	0.35	3.58	2.1	13.4	1.4
147165 H	B1III	0.34	6.249	0.36	3.808	0.27	6.24	1.6	17.6	1.0
147889 H	B2III/IV	1.04	38.14	1.96	112.70	3.71	54.3	3.7	33.4	2.1
148184 H	B2Vnec	0.48	13.82	0.97	36.01	1.41	20.1	2.1	13.3	1.5
152233 H	O6III	0.42	26.58	0.48	14.55	0.51	13.7	2.2	19.8	1.3
152235 H	B0.7Ia	0.78	57.71	0.27	38.42	0.20	18.0	0.6	35.8	1.4
152249 H	O9Ib	0.48	21.04	0.27	13.84	1.57	12.5	3.0	19.7	1.4
163800 H	O7	0.57	16.73	1.48	33.46	1.48	24.2	3.0	27.7	1.5
179406 H	B3V	0.31	3.598	0.43	19.95	0.44	20.6	1.9	20.0	1.1
147933 H	B2V	0.45	16.25	0.47	23.46	0.44	22.1	2.0	16.7	1.7
110432 U	B2pe	0.48	16.88	0.10	15.92	1.00	6.7	0.6	17.5	0.7
152236 U	B1Iape	0.65	21.75	0.20	26.22	0.21	17.6	1.0	35.8	1.1
152424 U	O9Iab	0.63	43.49	0.21	25.09	0.25	17.0	1.0	39.7	4.6
35149 U	B2V	0.16	11.48	0.14	5.23	0.12	1.8	0.7	9.6	7.8
37903 U	B2V	0.31	12.12	0.19	7.97	0.25	2.9	1.4	28.9	8.4
52266 U	O9V	0.24	14.67	0.33	5.07	0.54	6.5	1.6	19.0	7.2
52382 U	B1Ib	0.39	22.51	0.12	8.53	0.16	7.8	0.6	23.7	2.6
53974 U	B0.5IV	0.28	13.93	0.10	5.67	0.12	3.5	0.4	15.7	1.8
58510 U	B1Ia	0.30	12.89	0.15	5.67	0.19	5.2	0.9	30.0	10.6
73882 U	O8V	0.67	22.25	0.32	33.48	0.22	7.7	0.7	18.1	5.6
75149 U	B3Ia	0.40	12.21	0.12	9.14	0.11	7.2	0.4	25.4	1.7
76341 U	O9III	0.54	53.43	0.28	35.74	0.35	9.9	0.7	22.2	2.0
91452 U	B0III	0.55	10.54	0.21	27.16	0.26	10.9	0.6	30.1	8.6
92964 U	B2.5Iae	0.37	9.647	0.12	12.69	0.16	12.3	0.6	30.3	1.9
148379 U	B2Iab	0.77	22.37	0.48	17.60	0.77	10.7	1.5	43.2	1.4
149404 U	O9Ia	0.62	49.50	0.46	28.63	0.32	17.6	1.7	41.1	0.9
151932 U	WN7	0.50	15.01	0.34	31.61	0.87	16.7	1.4	29.5	1.0
154445 U	B1V	0.35	21.02	0.31	19.53	0.40	10.6	1.8	22.8	0.8
148688 U	B1Ia	0.52	28.39	0.80	15.54	0.69	10.0	1.7	37.4	1.6
152270 U	WC7	0.50	20.68	0.69	14.27	1.15	10.8	5.1	16.4	2.0
115363 U	B1Ia	0.81	21.32	1.24	34.14	1.36	32.1	4.9	—	—
136239 U	B2Iae	1.08	53.97	1.15	25.63	1.42	20.5	6.3	31.7	2.6
154368 U	O9.5Iab	0.73	21.11	0.26	58.94	0.15	20.7	0.6	27.8	0.9
157038 U	B4Ia	0.85	62.35	0.29	21.20	0.31	7.7	0.9	47.7	1.8
161056 U	B3Vn	0.55	24.43	0.26	53.26	0.20	28.6	0.6	36.2	2.7
169454 U	B1Ia	1.11	20.91	0.28	36.74	0.17	25.8	0.6	54.0	3.2
170740 U	B2V	0.45	16.80	0.11	19.86	0.10	6.0	0.4	24.5	0.9
149757 U	O9.5V	0.28	30.71	0.12	23.86	0.07	7.33	0.5	9.8	1.1
210121 U	B3V	0.32	12.36	1.04	35.20	1.91	14.4	4.1	10.7	3.7